Int. J. Electrochem. Sci., 12 **(2017)** 6445 – 6464, doi: 10.20964/2017.07.66

International Journal of ELECTROCHEMICAL SCIENCE
www.electrochemsci.org

Degradation Kinetics of 4-chlorophenol Wastewater and Toxicity Evolution in the Process of Electrochemical Reduction-Oxidation Coupling under Three-Electrode Diaphragm System

Dandan Xu[1], *Yan Wang*[1], *Hui Wang*[1,*], *Zhaoyong Bian*[2,*]

[1] College of Environmental Science and Engineering, Beijing Forestry University, Beijing 100083, PR China
[2] College of Water Sciences, Beijing Normal University, Beijing 100875, PR China
[*]E-mail: wanghui@bjfu.edu.cn, bian@bnu.edu.cn

Received: 7 April 2017 / *Accepted:* 14 May 2017 / *Published:* 12 June 2017

Electrochemical reduction-oxidation process was used to degrade simulated paper wastewater using three-electrode diaphragm system with Pd-Fe/graphene gas-diffusion cathode. The degradation efficiency and toxicity variation assessment were analyzed during the 4-chlorophenol (4-CP) wastewater degradation process. The 4-CP wastewater was degraded effectively and the removal efficiency of chemical oxygen demand (COD) in simulated paper wastewater was 78.2% (anodic), 80.7% (cathodic 1) and 81% (cathodic 2). The toxicity inhibition effect of two cathodic and anodic almost reached 100%, 100%, and 81.0% at 120 min, respectively. The comparison showed concentration for 50% of maximal effect (EC_{50}) of simulated paper wastewater increased with the raise of EC_{50} of 4-CP. The elimination of toxicity exhibited a hysteresis effect and a rise tendency within 60 min, which might be attributed to the formation of more toxic intermediates such as benzoquinone. A good kinetics model was used to predict degradation of 4-CP and two possible reaction pathways were proposed, featuring a series of steps including cleavage of C-Cl bond, hydrodechlorination, hydroxyl radical addition and oxidation. The Pd-Fe/graphene gas-diffusion cathode was promising to dechlorination and detoxication of simulated paper wastewater containing 4-CP.

Keywords: simulated paper wastewater; 4-chlorophenol; reduction-oxidation process; kinetics; toxicity

1. INTRODUCTION

Paper industry is one of the largest water polluters in the world. Paper production has globally increased and will continually increase in the near future [1]. Owing to active chlorinate is used in

bleaching process, paper wastewater produces a large number of chlorinated organic compounds, especially the chlorinated phenols, that are the main components of persistent organic pollutants (POPs). The chlorinated phenols compounds include 4-chlorophenol (4-CP), 2,4-dichlorophenol, 2,4,6-trichlorophenol, and pentachlorophenol etc. [2]. Chlorophenols are ubiquitous in various industrial wastewater, such as manufactures of preservatives, pesticides and dyes, and pulp and paper industries [3, 4]. 4-CP has been listed as a priority pollutant due to their teratogenic, carcinogenic, mutagenic, persistence and high toxicity [5-7]. 4-chlorophenol is difficult to the natural- and bio-degradation because of their low water solubility and vapor pressure [8]. As a consequence of its wide usage and negative health impacts, it is necessary to develop efficient method to remove 4-CP simulated paper wastewater.

Various technologies have been mooted to eliminate paper wastewater in recent years. Although biodegradation is eco-efficient and environment friendly, it cannot effectively degrade organic compounds from toxic wastewater [9, 10]. With this context, electrochemical technologies have been regarded as great progress, especially for the treatment of biorefractory substances. The most important advantages of electrochemical methods for the treatment of wastewater are their high efficiency, mild operating condition, ease of automation, versatility, and low cost. The main electrochemical procedures utilize for the remediation of wastewater are electrocoagulation, electro-Fenton, electroreduction, electrochemical oxidation [11]. Electron-Fenton has been widely investigated for organic pollutants elimination in environment due to in-situ production of hydrogen peroxide [12]. Then combining with externally added Fe^{2+} as catalyst to produce hydroxyl radicals as main oxidizing agent. However, ferrous ions are destroyed easily by hydroxyl radicals and negatively affect the oxidation process [13]. Recently, electrochemical oxidation has been used for removal of organic pollutants, and achieves good results [14]. But it is difficult to achieve complete dechlorination and detoxification in chlorophenol organic compounds treatment process [15]. On the other hand, electrochemical reduction process has effectively decreased the toxicity of chlorinated organic wastewater, but it is incapable to achieve further degradation being applied simultaneously to treat organic intermediate products [16, 17]. In comparison with anodic oxidation, cathodic reduction dechlorination on the cathode surface is usually faster and more cost-effective than that by anodic oxidation [18, 19]. As the unique properties as handling convenience, rapidness, high sensitivity, automatics and low-cost equipment, electrochemical reduction-oxidation process has received increasing attention in the pollutants treatment [20, 21]. There have been many reports regarding the catalyst material on the electrode surface during dechlorination, especially nanostructured Pd, has been found to exhibit excellent catalytic by adsorbing hydrogen to produce a reduction under mild reaction conditions [22]. Furthermore, the present of Fe plays a significant role in the production hydrogen, which might be collected by Pd to form adsorbing hydrogen, and Fe also performs direct reductive dechlorination [23]. The Pd-Fe bimetallic catalyst also allow a lower-cost means of degrading chlorophenols.

Since the intermediate products originating from 4-CP degradation might be more toxic and cause secondary pollution, it is necessary to determine the intermediates and their associated toxicity [24]. The present work optimized experimental conditions and evaluated toxicity of intermediates or CPs without considering toxicity variation even though this information was important for

environmental protection [25]. Moreover, kinetics study contribute to further understanding the degradation pathway and mechanism toward electrochemical reduction-oxidation of 4-CP. Therefore, degradation pathway, the kinetics and toxicity assessments of simulated paper wastewater containing 4-CP degradation process still deserve to be investigated systematically during electrochemical reduction-oxidation.

The aim of the present study was to provide a thorough investigation of simulated wastewater containing 4-CP electrochemical reduction-oxidation degradation focusing on: (1) to identify degradation efficiency and toxicity change of simulated paper wastewater, (2) to compare toxicity variation between simulated paper wastewater and 4-CP during the electrolysis process, (3) to study the kinetics of 4-CP and propose the possible degradation pathway of 4-CP.

2. MATERIAL AND METHODS

2.1 Simulation of paper wastewater containing 4-CP

Paper wastewater production from pulp and paper plant is generally associated with ketones, acids and chlorinated organic compounds and other aromatic compounds, especially chlorophenols [26]. The present study chose acetovanillone, 4-chlorophenol, 2-methyl acetone, and alanine as pollutant components of simulated paper wastewater. The content of composition in simulated wastewater is showed in Table 1.

Table 1. Composition and content of simulated wastewater

Substance	Acetovanillone	4-CP	2-methyl acetone	Alanine
Concentration (mg L^{-1})	126	26.4	23.8	18

2.2 Electrolysis experiments procedures

With two organic diaphragms (Tangshan Fengrun Jinxiang Chemical Fiber Co., Ltd, China), a $Ti/IrO_2/RuO_2$ anode (Wuhan Kaida Technology Engineering Co., Ltd, China), and two self-made Pd-Fe/graphene gas-diffusion cathodes, the simulated paper wastewater and 4-CP degradation was investigated by a combination process of electrochemical reduction and electrochemical oxidation. The preparation of Pd-Fe/graphene catalyst was performed by photo-induced reduction method, and exhibited the optimal surface performance by X-ray diffraction, transmission electron microscopy, X-ray photoelectron spectroscopy characterization and high electrocatalytic activity by electrochemical measurement using CHI-660d workstations [27]. The electrochemical degradation reactor was reported elsewhere [20]. The volume of electrolytic reactor was 12 cm (length) ×6 cm (width) ×7.5 cm (height), the space between the electrodes was 2 cm. 150 mL of simulated paper wastewater was prepared according section 2.1. The concentration of individual 4-CP in 0.03 mol L^{-1} Na_2SO_4 supporting electrolyte was 100 mg L^{-1}. Then, the synthetic solution was transferred into the electrochemical

reactor. The optimal operating parameters were the initial pH value of 7.0, current density of 25 mA cm^{-2} and reaction time of 120 min according previous study. The initial pH of the solution was adjusted using sodium hydroxide and hydrochloric acid. Before starting electrolysis, hydrogen gas was fed for 5 min with the rate of 25 mL s^{-1} to keep dissolved gas saturation. Hydrogen gas was then fed into the gas compartment during 0-60 min (electrolysis time), following air.

2.3 Analytical methods

2.3.1 Toxicity measurement

The toxicity testing was evaluated whether the transformation products formed had higher toxicity than the parent compound [28]. The acute toxicity of degradation process was assessed using the luminescent freshwater bacteria, photobacterium phosphoreum. The freeze-dried powders of photobacterium phosphoreum were purchased from the institute of Soil science, Chinese Academy of Sciences (Nanjing, China). The freeze-dried powder was rehydrated using 2 mg 100 ml^{-1} NaCl before testing. The temperature of test was 20 °C. The values of toxicity were presented as the concentration for 50% of maximal effect (EC_{50}).

When the luminescent bacteria are exposed to toxic substances, the bacterial luciferase is inhibited and light intensity decrease rapidly [29]. The toxicity effects were expressed as EC_{50} that was the concentration of toxicant corresponding to the inhibition value of 50% at a 15 min of exposure time [30]. The samples for toxicity test were diluted in Milli-Q water to different concentration gradient. The endpoint of toxicity was the measurement of bioluminescence reduction. The toxicity value was calculated by Eq. (1)

$$I(\%) = \frac{L_B - L_S}{L_B} \times 100\% \quad (1)$$

Where I represents the inhibition of the concentrated sample to luminescent bacteria. L_B is the blank luminescent intensity. L_S is the samples luminescent intensity.

Concentration addition (CA) is based on the assumption that mixture component have the same sites and similar mode of action. To predict the effect of a mixture of chemicals with same mode of action, the CA model could be written as Eq. (2) [31].

$$ECx_{mix} = \left(\sum_{i-1}^{n} \frac{P_i}{EC_{X_i}}\right)^{-1} \quad (2)$$

Where $P_i = C_i / C_{mix}$ is the concentration C_i expressed as relative proportion of the total concentration $C_{mix} = \sum C_i$.

2.3.2 Other measurements

To determine the concentration variation of 4-CP, samples were analyzed by high performance liquid chromatography (HPLC, Waters, USA). HPLC equipped with ODS-SP C18 separation column using a mobile phase of methanol: water (80:20, v/v) at a flow ratio of 1.0 mL min^{-1}. The column temperature, injection volume, UV wavelengths were set at 35 °C, 30 μL, 230 nm and 280 nm.

The mineralization degree of 4-CP was determined with total organic carbon (TOC) measurements performed by Shimadzu TOC-5000 analyzer. The concentration of chemical oxygen demand (COD) in simulated paper wastewater was measured using COD measuring instrument (Lianhua technology, China) during electrochemical process.

3. RESULT AND DISCUSSION

3.1 Degradation and toxicity analysis of simulated paper wastewater

The electrochemical oxidation-reduction degradation of simulated paper wastewater of 4-CP, which was prepared according to section 2.1, was performed using Pd-Fe/graphene cathode and $Ti/IrO_2/RuO_2$ anode under optimal conditions. The original COD of simulated paper wastewater was 550 mg L^{-1}. The removal efficiency of COD with reaction time was achieved in different electrode compartments (Fig. 1a).

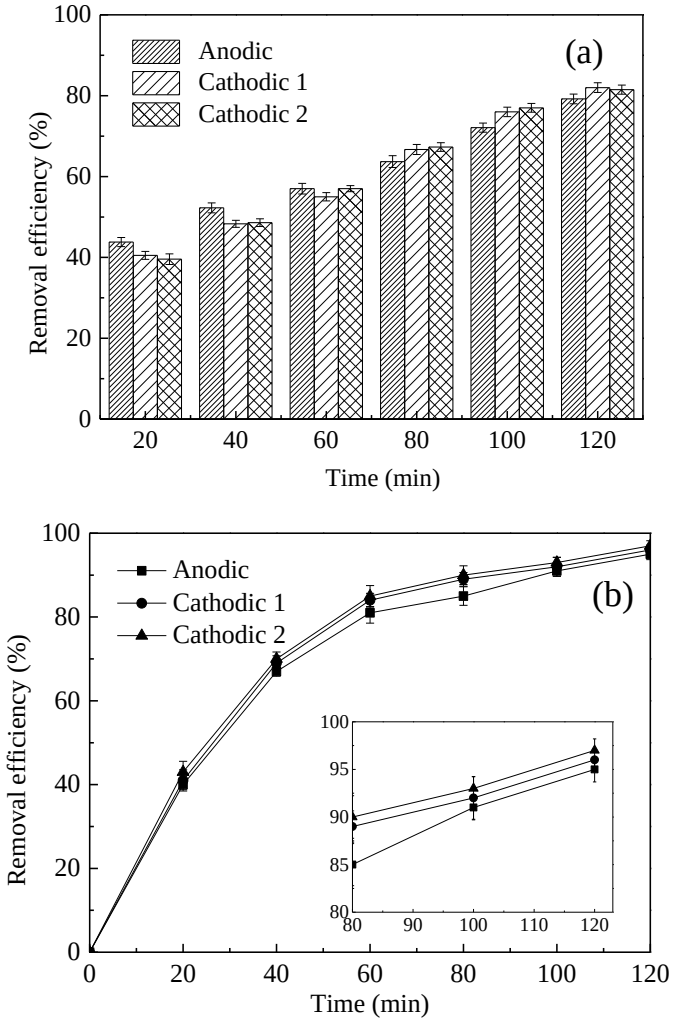

Figure 1. Removal of COD (a) in simulated wastewater and 4-CP (b) in the two cathodic and anodic compartments with electrolysis time at feeding hydrogen and air by the Pd-Fe/graphene gas-diffusion electrode system. Initial pH: 7.0. Current density: 25 mA cm^{-2}. Electrolyte: 0.03 mol L^{-1} Na_2SO_4. The insert (b) shows enlarged picture of removal efficiency in the 80-120 min

The COD removal increased constantly in two cathodic and anodic compartments with electrolytic reaction process. At 60 min, the removal rate reached about 50%. And the end of the electrolysis reaction, the COD elimination rates in anodic compartment, cathodic compartment 1 and cathodic compartment 2 were 78.2%, 80.7%, and 80.1%, respectively. It proves electrochemical reduction-oxidation process is effective to remove organic matter and reduce the concentration of COD in simulated paper wastewater.

The removal efficiency of 4-CP in simulated paper wastewater was investigated in different electrode compartments and the result is presented in Fig. 1b.

It had high removal efficiency of simulated wastewater containing 4-CP in different electrode compartments. The concentration of 4-CP in simulated paper wastewater decreased with the reaction time, the removal efficiencies of cathodic 1, cathodic 2 and anodic compartment were 96.8%, 96.4% and 95.3% after 120 min, respectively. And degradation efficiency using Pd-Fe/graphene cathode was obviously higher than that using Pd/graphene (89.6%) and Pd/RGO/foam-Ni cathode (95.1%) in the cathodic compartment at 120 min reported by Liu and Wang [20, 32], it proved Pd-Fe/graphene cathode was more suitable and promising to 4-CP degradation. And in the whole electrolysis process, the conversion rate in the cathodic was higher than that of the anodic. It was suggested that during the first 60 min, -Cl was replaced by an active hydrogen species to generate Cl^- with hydrogen gas feeding using Pd-Fe/graphene gas diffusion cathode. The catalyst Pd-Fe/graphene was used for the hydrodechlorination of 4-CP. Then the cathodic compartment produced H_2O_2 as a result of exist of air after 60 min. And H_2O_2 was decomposed into hydroxyl radial (HO·) and O^{2-}· [20]. The HO··serves strong oxidizing property [33]. The Pd-Fe/graphene catalyst improved reduction ratio of O_2 to H_2O_2 in the air feeding. In anodic compartment, MO_x(·OH) or MO_{x+1} seems to be involved in anodic indirect electrochemical oxidation, but it is difficult to achieve high removal efficiency because of low MO_x(·OH) or MO_{x+1} concentration on the anode [17]. However, the oxidizing ability of H_2O_2 was strong during oxygen reduction on Pd-Fe/graphene gas diffusion electrode, HO· oxidized organic pollutants to smaller molecule products. The result indicates that Pd-Fe/graphene gas-diffusion cathode has strong electrocatalytic ability for 4-CP in simulation paper wastewater.

As we all known, 4-CP is high toxic substance and has potential risk on aquatic ecosystem. In order to evaluate the main toxic effect of 4-CP to simulated paper wastewater and toxicity pattern of the reaction system, the toxicity changes of simulated paper wastewater and individual 4-CP during electrochemical oxidation-reduction degradation process are compared in Fig. 2. Then the EC_{50} of initial simulated paper wastewater was 51.0% (Fig. S1).

As can be observed in Fig. 2, EC_{50} of simulated paper wastewater in anodic compartment decreased from 11.7% to 7.8% when the degradation time from 20 min to 40 min. Then, EC_{50} increased with the degradation reaction, and the value was 81.0% at 120 min. The result indicated the toxicity of paper wastewater increased first and then decreased until low toxic with degradation process. Perhaps it was because the primary toxicity to luminescent bacteria came from more toxic substance, such as benzoquinone, it was oxidation intermediate product of 4-CP and its toxicity was higher than that of 4-CP [34, 35]. Subsequently, benzoquinone was degraded into small molecule acids to reduce toxicity. Different from the toxicity of anodic, the EC_{50} of simulated paper wastewater increased constantly and reached the biggest value of EC_{50} in double cathodic compartments. The EC_{50}

in two cathodic were approximately 100% at 120 min. It demonstrated that paper wastewater was degraded into lower toxic products in cathodic compartments using Pd-Fe/graphene gas diffusion cathode. The chlorine substituent in the organic compounds contributes to the toxicity of aromatic compound. Therefore, it proves Pd-Fe/graphene gas-diffusion cathode is more suitable to reduction dechlorination and fast oxidation organic pollutant in simulated paper wastewater without high toxic products.

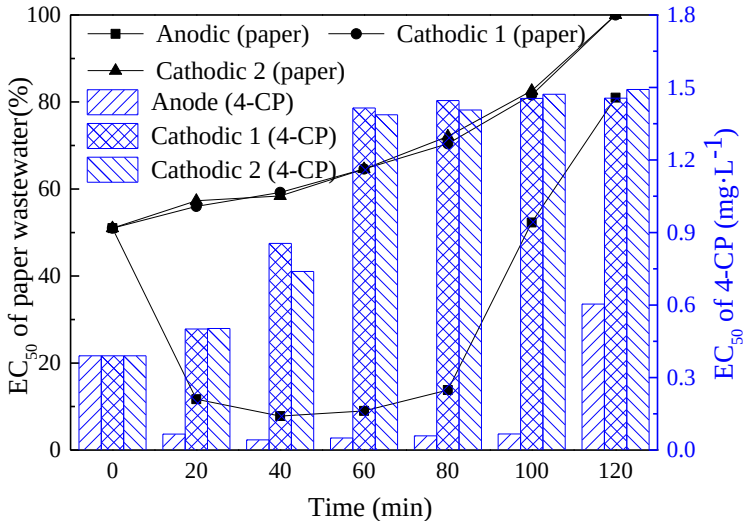

Figure 2. Evolution of toxicity of simulated paper wastewater (black line) and 4-CP (blue bar) with electrolysis time during electrochemical reduction-oxidation process in terms of percentage and concentration of inhibition of photobacterium phosphoreum after 15 min of exposure in different electrode compartment. Current density: 25 mA cm^{-2}. Electrolyte: 0.03 mol L^{-1} Na_2SO_4. Initial pH: 7.0

Moreover, the mixture toxicity of 4-CP degradation process with electrolysis time were also calculated and analyzed. The EC_{50} of 4-CP at constant time intervals was calculated according the Eq. (2). It decreased from 0.39 mg L^{-1} to 0.042 mg L^{-1} within 40 min, the increased inhibitions should be related to the generation of benzoquinone, resulting in the toxicity effect of 4-CP wastewater [35]. The EC_{50} of 4-CP in cathodic compartments increased constantly in the whole electrochemical degradation process caused by the reduction dechlorination products produced firstly using Pd-Fe/graphene cathode. Furthermore, benzoquinone was not detected in cathodic, and toxicity was decreased with the removal of 4-CP parent molecular. That suggested the cathodic compartments achieved good degradation and detoxification using Pd-Fe/graphene gas-diffusion cathode.

The comparison between simulated paper wastewater and individual 4-CP showed EC_{50} (%) of simulated paper wastewater increased with the increase of EC_{50} of 4-CP, and both variation trends were consistent. When the toxicity of 4-CP was reduced to a minimum, and that of simulated paper wastewater also reached the lowest in three-electrode system, when the toxicity of 4-CP was maximum value at 60 min in the anodic compartment, that of simulated paper wastewater also reached the highest at same time. The result indicated toxicity change of simulated paper wastewater was mainly affected by the toxicity of 4-CP, that is to say, 4-CP was one of the most important contaminants in

simulated paper wastewater. Thus, it is significant to study the degradation pathways and kinetics of individual 4-CP in electrochemical reduction-oxidation process.

3.2 Degradation pathway of individual 4-CP

The identification of intermediates from electrochemical reduction oxidation of 4-CP using Pd-Fe/graphene cathode was evaluated by gas chromatography and mass spectrometer. And the concentration of 4-CP and intermediates were determined using HPLC and IC, and the results were shown in the previous reports [34], such as phenol, benzoquinone, hydroquinone, formic acid, acetic acid, succinic acid, and fumaric acid. A comparison of the measured TOC values and bound carbon values calculated from the concentration of the 4-CP and the intermediates (C_{cp+Int}) with electrolysis time are presented in Fig. 3.

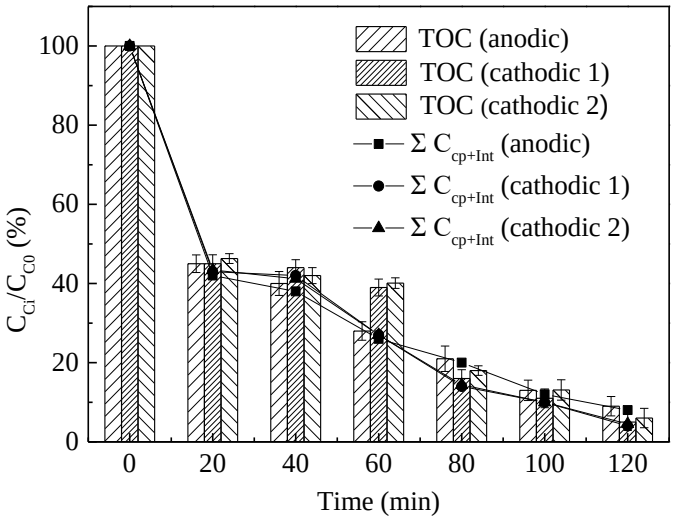

Figure 3. Concentration variation of TOC (bars) and 4-CP and main intermediates (lines) in two cathodic and anodic compartments using Pd-Fe/graphene cathode at current density of 25 mA cm^{-2} within 120 min. The solution contained 0.03 mol L^{-1} Na_2SO_4 at pH 7.0. Initial concentration of 4-CP: 100 mg L^{-1}

As TOC removal reflects the mineralization of organic compounds, the variation of TOC was measured during electrochemical treatment [36]. Fig. 3 shows a high mineralization degree of 4-CP. The TOC removal efficiency after 120 min in two cathodic compartments and anodic compartment were 92.8%, 91.6% and 91.4%. TOC removal was almost 100% and mineralized to CO_2 and H_2O. In addition, if intermediate products were all detected, the concentration ratio of ΣC_{cp+Int} and TOC was almost same. Fig. 3 shows that concentration ratio of ΣC_{cp+Int} was only slightly less than that of TOC in three-electrode system, the ratio of ΣC_{cp+Int} and TOC all reached about 80%. It indicated most of intermediate products had been already detected and could accurately infer reaction process. Also, due to benzene ring structure were not been damaged in 60 min in cathodic that mainly carried out dechlorination, so the concentration of TOC was higher than that of anodic.

Based on the structure elucidation of degradation products, possible electrochemical degradation pathway of 4-CP under Pd-Fe/graphene gas-diffusion cathode and Ti/IrO_2/RuO_2 anode was proposed. After considering the experimental results analyzed above, Fig. 4 shows possible reaction pathway for 4-CP degradation.

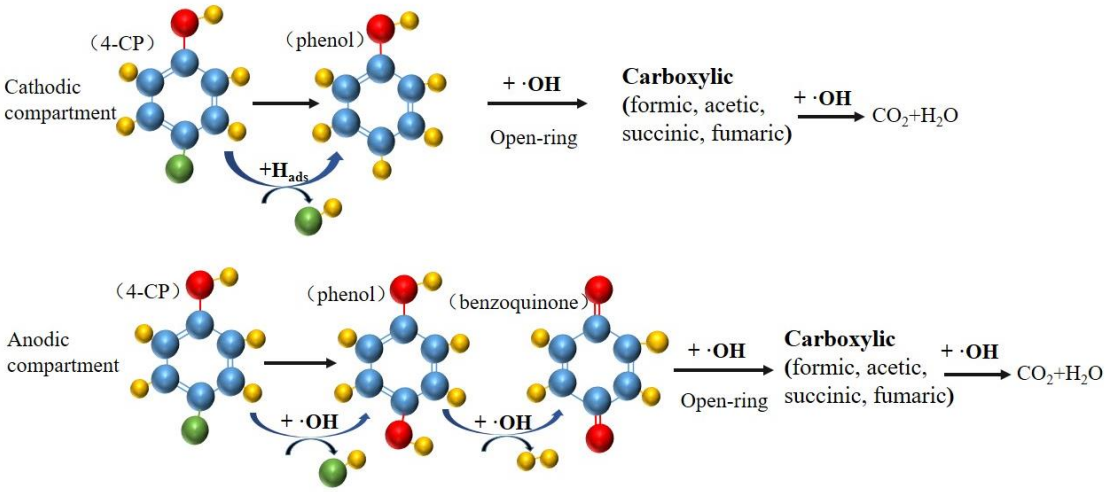

Figure 4. Proposed degradation pathways for 4-CP in electrochemical reduction-oxidation process in cathodic and anodic compartments using Pd-Fe/graphene gas-diffusion electrode. Current density: 25 mA cm^{-2}. Electrolyte: 0.03 mol L^{-1} Na_2SO_4. Initial pH: 7.0

There were two degradation processes of 4-CP in cathodic compartment and anodic compartment under the electrochemical reduction-oxidation process. The one pathway which happened in cathodic compartments was that hydrodechlorination of 4-CP to produce phenol, then hydroxyl radial attacked on para position of phenol to form hydroquinone. The attributed to the fact that H_2 was fed into the Pd-Fe/graphene gas-diffusion electrode system at first 60 min and hydrogen atoms were generated on the electrode surface. Then chlorine atoms were replaced by the hydrogen atoms, giving hydrodechlorination of 4-CP, but slow mineralization. This active hydrogen atoms were responsible for the hydrodechlorination of 4-CP [37]. Hydrogen atoms provided reduction driving force and made the C-Cl cleavage in cathodic compartments [38]. Then aromatic intermediates were oxidized to carboxylic acids, because they reacted rapidly with the large amount of HO· formed from the reduction of O_2 by feeding of air. But this process was fast, so they weren't been detected in the solution besides phenol and carboxylic. Another pathway in anodic compartment found that 4-CP directly was attacked by hydroxyl radial to form hydroquinone. Then, hydroquinone was oxidized to benzoquinone by hydroxyl radial and continuously oxidized to carboxylic acids due to its extremely strong oxidation capacity. The aromatic oxidation products included benzoquinone, hydroquinone and phenol were detected in anodic compartment. The results indicated the Pd-Fe/graphene could promoted hydrogenolysis to replace the chlorine atom in a chlorinated organic compound with a hydrogen atom at first 60 min. After 60 min, it catalyzed and accelerated the two-electron reduction of O_2 to H_2O_2 and peroxide anion (HO_2^-), which might be converted to strong oxidants [23].

3.3. Kinetics study for 4-CP degradation

3.3.1 Kinetics model

4-CP degradation is dependent on both the process of the electrochemical oxidation and electrochemical reduction. It is necessary to discuss the optimizing design and step in the combined degradation process by means of kinetics model. The 4-CP degradation process showed that it probably proceed through three steps in anodic and cathodic compartment according degradation pathway, respectively. Fig. 5 represents the principal steps of 4-CP degradation on the basis of the main intermediates products. That might exist the electrochemical reduction oxidation of 4-chlorophenol to organic acids through and not through quinonic compounds simultaneously. According to the main reaction pathway of anodic and cathodic compartment, degradation reaction rate constant (K) of chlorophenol, aromatic or phenol and organic acids were obtained.

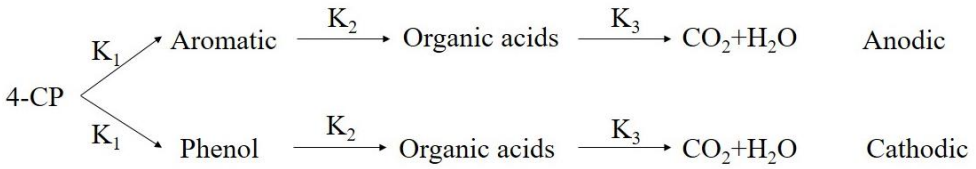

Figure 5. Principal pathways of 4-CP degradation by electrochemical reduction-oxidation process in cathodic and anodic compartments

The following set of differential equations could be obtained according to the reaction diagram in anodic compartment:

$$\frac{d[R_{A1}]}{dt} = -K_1[R_{A1}] \quad (3)$$

$$\frac{d[R_{A2}]}{dt} = -K_2[R_{A2}] + K_1[R_{A1}] \quad (4)$$

$$\frac{d[R_{A3}]}{dt} = K_2[R_{A2}] - K_3[R_{A3}] \quad (5)$$

In the above reaction equations, K_i (i=1, 2, 3) is the apparent rate constant that 4-CP was degraded into aromatic organic, aromatic organic was degraded into organic acids and organic acids was degraded into CO_2 and H_2O. Where $[R_{A1}]$ represents the concentration of the 4-CP, $[R_{A2}]$ represents the concentration of aromatic intermediates, $[R_{A3}]$ represents the concentration of the carboxylic acids. The integration constant can be evaluated from the initial condition: At time $t = 0$, $[R_{A1}] = [R_{A1}]_0$, $[R_{A2}] = [R_{A3}] = 0$, $[R_{A1}]_0$ represents the initial concentration of 4-CP. The generalized kinetics model according the equations and conditions was given by:

$$[R_{A1}] = [R_{A1}]e^{-K_1 t} \quad (6)$$

$$[R_{A2}] = [R_{A1}]\left(\frac{K_1}{K_2 - K_1}\right)\left(e^{-K_1 t} - e^{-K_2 t}\right) \quad (7)$$

$$[R_{A3}] = [R_{A1}]\left[\left(\frac{K_1 K_2 e^{-K_1 t}}{(K_3 - K_1)(K_2 - K_1)}\right) + \left(\frac{K_1 K_2 e^{-K_2 t}}{(K_2 - K_1)(K_2 - K_3)}\right) - \left(\frac{K_1 K_2 e^{-K_3 t}}{(K_3 - K_1)(K_3 - K_2)}\right)\right] \quad (8)$$

According to the main reaction pathway of cathodic compartment, differential equations could be obtained that was similar to that of anodic compartment:

$$\frac{d[R_{C1}]}{dt} = -K_1[R_{C1}] \quad (9)$$

$$\frac{d[R_{C2}]}{dt} = -K_2[R_{C2}] + K_1[R_{C1}] \quad (10)$$

$$\frac{d[R_{C3}]}{dt} = K_2[R_{C2}] - K_3[R_{C3}] \quad (11)$$

In the above reaction equations, K_i (i=1, 2, 3) is the apparent rate constant for the combined process of 4-CP was degraded into phenol, phenol was degraded into organic acids and organic acids was degraded into CO_2 and H_2O. The integration constants can be evaluated from the initial condition, at time t = 0, $[R_{C1}] = [R_{C1}]_0$, $[R_{C2}] = [R_{C3}] = 0$, $[R_{C1}]_0$ represents the initial concentration of 4-CP. The generalized kinetics model was given by:

$$[R_{C1}] = [R_{C1}]e^{-K_1 t} \quad (12)$$

$$[R_{C2}] = [R_{C1}]\left(\frac{K_1}{K_2 - K_1}\right)\left(e^{-K_1 t} - e^{-K_2 t}\right) \quad (13)$$

$$[R_{C3}] = [R_{C1}]\left[\left(\frac{K_1 K_2 e^{-K_1 t}}{(K_3 - K_1)(K_2 - K_1)}\right) + \left(\frac{K_1 K_2 e^{-K_2 t}}{(K_2 - K_1)(K_2 - K_3)}\right) - \left(\frac{K_1 K_2 e^{-K_3 t}}{(K_3 - K_1)(K_3 - K_2)}\right)\right] \quad (14)$$

3.3.2 Kinetics of different 4-CP initial concentration

To verify the application of kinetics model, effect of different initial concentration (25 mg L^{-1}, 50 mg L^{-1}, 100 mg L^{-1}, 200 mg L^{-1}, 500 mg L^{-1}) of 4-CP was measured. The fitting degrees for 4-CP, aromatic and carboxylic are showed in Fig. 6 and Fig. S2-S5 in anodic and cathodic compartments for five initial 4-CP concentration. Obviously, it shows well-fitting degree between experiment data and the fitted lines of the kinetics model supports well the proposed degradation model. The symbols represent the experimental data, while the continuous lines represent the calculated curves fitted by the kinetics model that proposed in section 3.1.1. The fitting kinetics equations and correlation coefficients of 4-CP degradation of 100 mg L^{-1} are shown in Table S1.

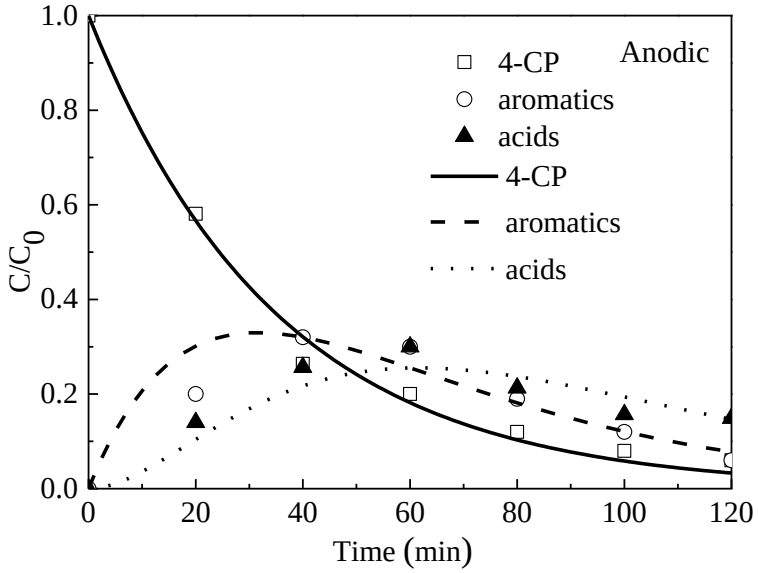

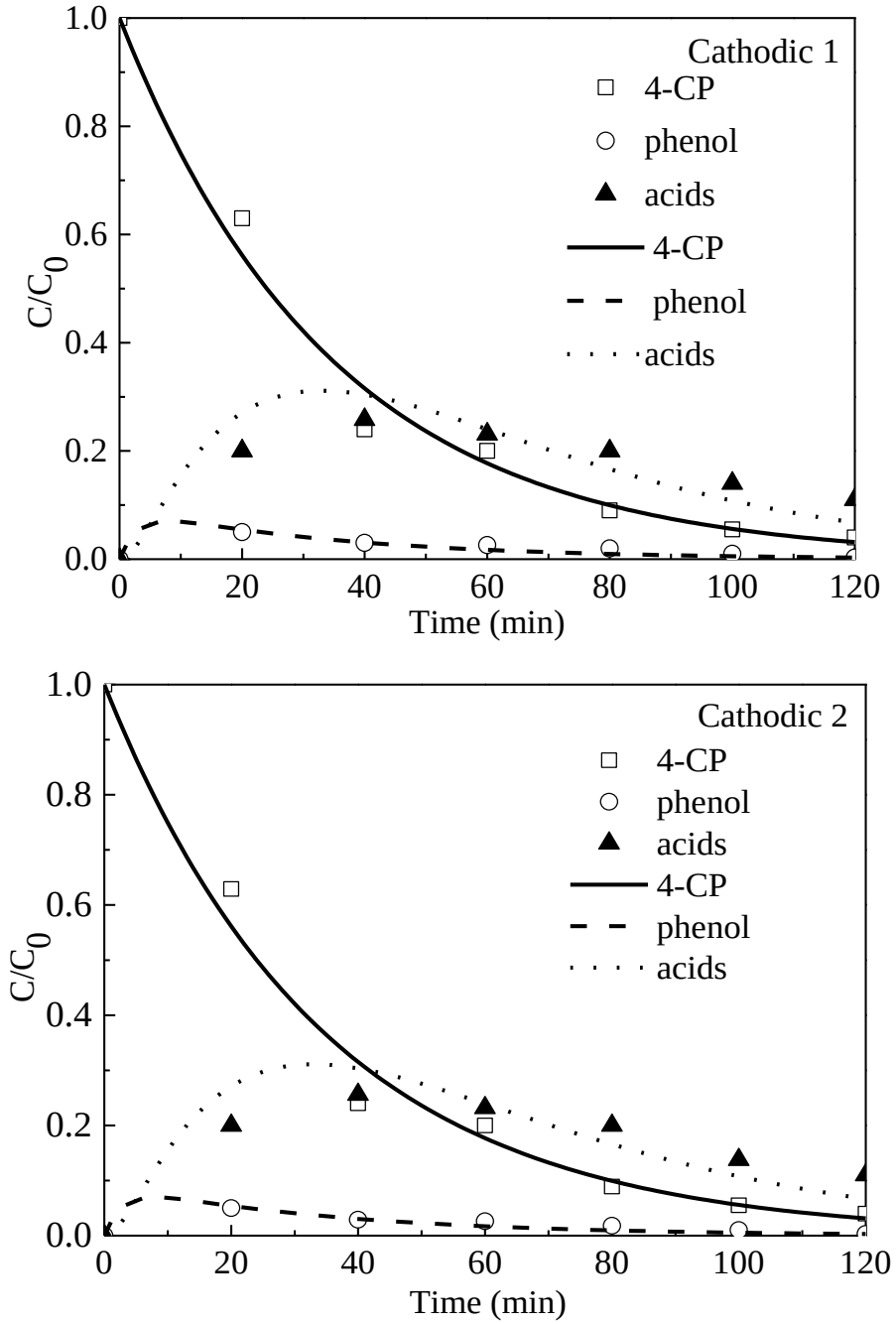

Figure 6. Experimental data (symbols) and model-fitting (lines) results of 4-CP, aromatics (phenol) and acids with electrolysis time during electrochemical reduction-oxidation process in two cathodic and anodic compartments. Initial concentration of 4-CP: 100 mg L^{-1}. Current density: 25 mA cm^{-2}. Electrolyte: 0.03 mol L^{-1} Na_2SO_4. Initial pH: 7.0

Obviously, as it was seen a good kinetics fitting effect between experimental and calculated curves fitted by the model was obtained for all the experimental series. The model could be used to predict degradation of 4-CP effectively at 25-500 mg L^{-1} of initial concentration.

Table 2. Apparent kinetics constant K_2 value obtained in the fit of the experiments at different initial concentration (25-500 mg L^{-1}) in the cathodic 1, cathodic 2 and anodic compartments

C ($mg \cdot L^{-1}$)	Cathodic 1	Cathodic 2	Anodic
25	0.379	0.381	0.0458
50	0.316	0.318	0.0371
100	0.324	0.328	0.0351
200	0.235	0.235	0.0322
500	0.168	0.169	0.0300

Table 3. Estimate apparent kinetics constant K_i values obtained in the fit of experiments in anodic, cathodic 1 and cathodic 2 compartments with initial concentration of 100 mg L^{-1} 4-CP

K_i	Anodic	Cathodic 1	Cathodic 2
K_1	0.0246	0.0288	0.0289
K_2	0.0351	0.324	0.328
K_3	0.0342	0.0392	0.0384

Table 2 and Table 3 list the kinetics parameters such as K_1, K_2 and K_3 of different electrode when the several initial concentrations of 4-CP are applied. It showed that apparent rate constant K_2 of the cathodic compartment 1 and cathodic compartment 2 were larger than that of the anodic. Other initial concentration of 4-CP also followed the same rule (Table S2-Table S5). It indicated that the ring opening of aromatics in the cathodic compartment was faster than anodic. 4-CP was degraded into less toxic organic acid using Pd-Fe/graphene gas-diffusion cathode. The conversion of 4-CP degraded into organic acid was not through benzoquinone or reaction immediately. However, K_2 decreased with the increase of the initial 4-CP concentrations in anodic and cathodic compartments. The phenomenon demonstrated that the aromatic intermediates were difficultly and slowly to be removed when the concentration of 4-CP was high. The result was similar to that of other literatures that high initial concentration of phenol results in the decrease of electrocatalysis performance [35, 39]. Besides, the value of K_1 in the cathodic compartments was greater than K_1 in the anodic when the initial concentration of 4-CP was less than 100 mg L^{-1}. It was proved that cathodic reduction dechlorination was prevailing step, which was superior to anodic oxidation when low concentration of 4-CP was applied. Moreover, the apparent kinetics constants K_2 both cathodic and anodic compartments were bigger than K_1 and K_3, it stated clearly that the second step that the aromatics were opened ring to organic acid was faster than the first step that 4-CP was degraded to aromatics and the third step that organic acids were converted into carbon dioxide and water. Similar K values trend was obtained in advanced electrochemical oxidation processes, but different from that of p-nitrophenol removal in electrochemical and adsorption combined process [40]. The reason was that adsorption process was usually to transfer rather than minimize contaminations. The electrochemical reduction-oxidation system showed better properties due to more rapid removal and bigger reaction kinetics constants (K_2) of generated intermediates regarded to electrochemical oxidation, electrochemical dechlorination, photolysis and photo-Fenton techniques. Comparison of the apparent kinetics rate constants of

chlorophenol electrochemical reduction oxidation process to that of other processes from literatures was summarized in Table 4. It showed that the 4-CP electrochemical reduction-oxidation was high competitive and promising. Consequently, the electrochemical system both cathodic chambers and anodic could be well used for opening ring to reduce toxicity for degrading 4-CP.

Table 4. Comparison of apparent kinetic rate constants of several treatment processes for degradation of phenols in different initial concentration

Pollutants	Initial concentration/ $mg \cdot L^{-1}$	Treatment conditions	K_1+K_2		Ref.
			K_1	K_2	
Phenol	60	photo-Fenton	0.0800	0.0424	[39]
	100	electrochemical oxidation	0.0261	0.0133	[35]
	200	electrochemical oxidation	0.0123	0.0595	[35]
2-CP	40	UV/H_2O_2 pH=7	0.0341	0.00258	[41]
	40	UV/H_2O_2 pH=3	0.0214	0.000392	[41]
4-CP	30	catalytic dechlorination	0.0103	0.00330	[42]
	25	electrochemical reduction-oxidation	0.0322	0.379	This work
	50		0.0311	0.316	This work
	100		0.0288	0.324	This work
	200		0.0230	0.235	This work
	500		0.0218	0.169	This work
	100	UV/O_3 pH=6	0.0118		[43]
	100	UV/O_3 pH=9	0.0249		[43]
PNP	150	electrochemical oxidation	0.0660	0.0200	[40]
	500	electrochemical oxidation	0.107	0.00800	[40]

4. CONCLUSION

The present experimental study primarily aimed at investigating acute toxicity and kinetics constants during electrochemical reduction-oxidation of 4-CP in simulated paper wastewater. The electrochemical reduction-oxidation process provided complete 4-CP removal and partial COD abatement in simulated paper wastewater during 120 min. The Pd-Fe/graphene cathode exhibited higher 4-CP and TOC removal rate than anode. The toxicity in the process of electrochemical reduction-oxidation was assessed by luminescent bacteria, which revealed that electrochemical reduction-oxidation was an efficient process for toxicity reduction, and Pd-Fe/graphene cathode showed a more promising electrode for toxicity removal. Different from that of anodic compartment, benzoquinone was not detected in cathodic compartments due to the reduction dechlorination and oxidation immediately. The kinetics model of 4-CP stated clearly that the aromatics were opened ring to form organic acid (K_2) was faster than 4-CP was degraded to aromatics (K_1) and organic acids were converted into carbon dioxide and water (K_3). The apparent rate constants K_2 in the cathodic compartment 1 and cathodic compartment 2 were larger than that of the anodic. The Pd-Fe/graphene gas-diffusion cathode in three-electrode system is promising to dechlorination and decrease toxicity of simulated paper wastewater containing 4-CP.

SUPPLEMENTARY MATERIAL:

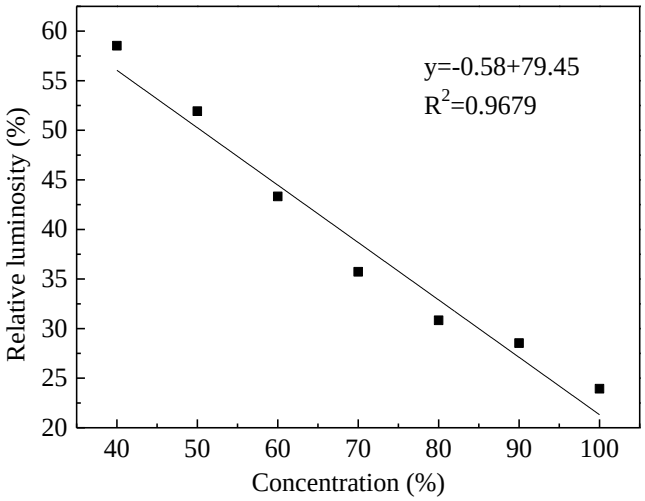

Fig. S1 Concentration relationship of simulated paper wastewater to inhibition percentage of photobacterium phosphoreum after 15 min of exposure

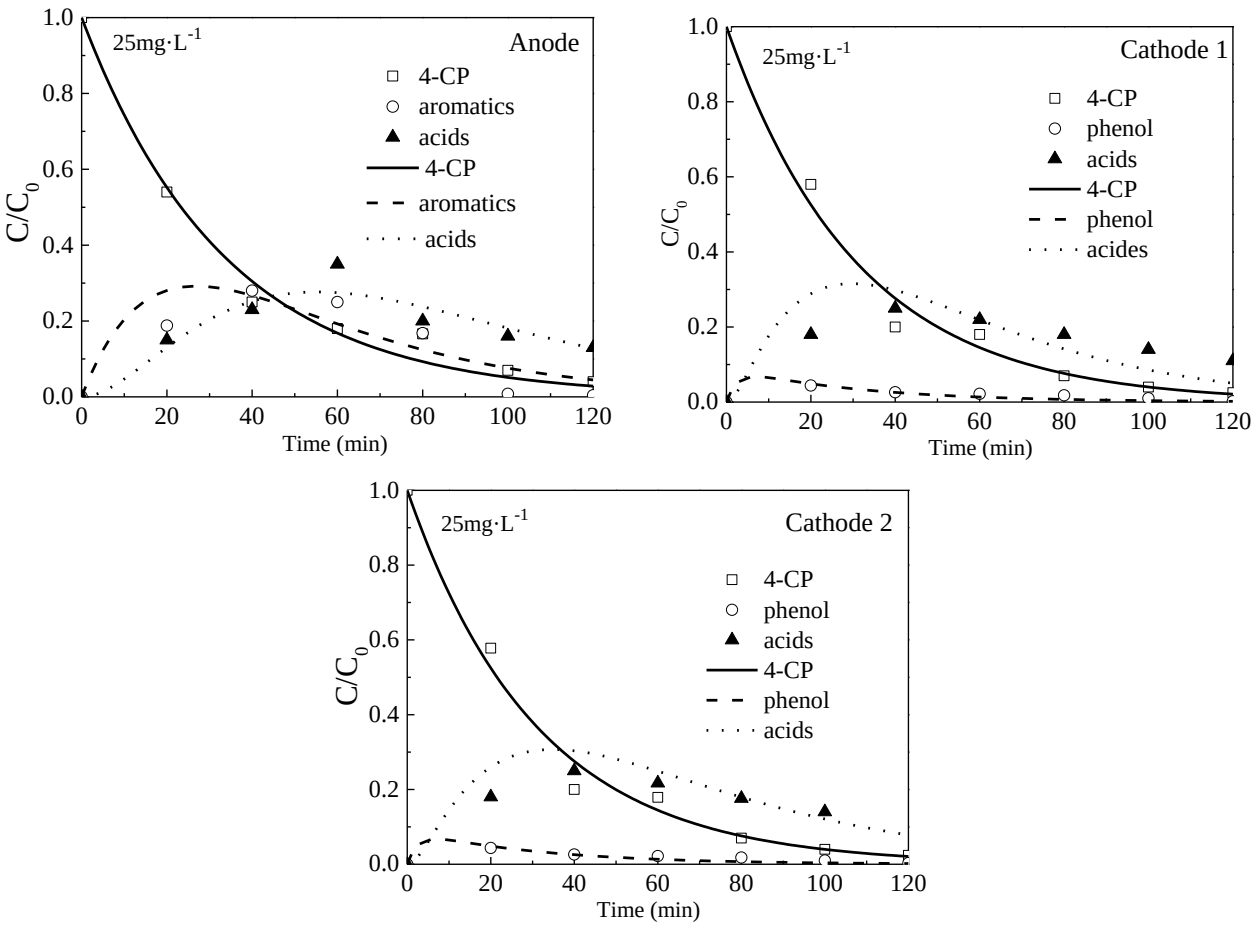

Fig. S2 Experimental data (symbols) and model-fitting (lines) results of 4-CP, aromatics (phenol) and acids with electrolysis time during electrochemical reduction-oxidation process in two cathodic and anodic compartments. Initial concentration: 25 mg L^{-1}. Current density: 25 mA cm^{-2}. Electrolyte: 0.03 mol L^{-1} Na_2SO_4. Initial pH: 7.0

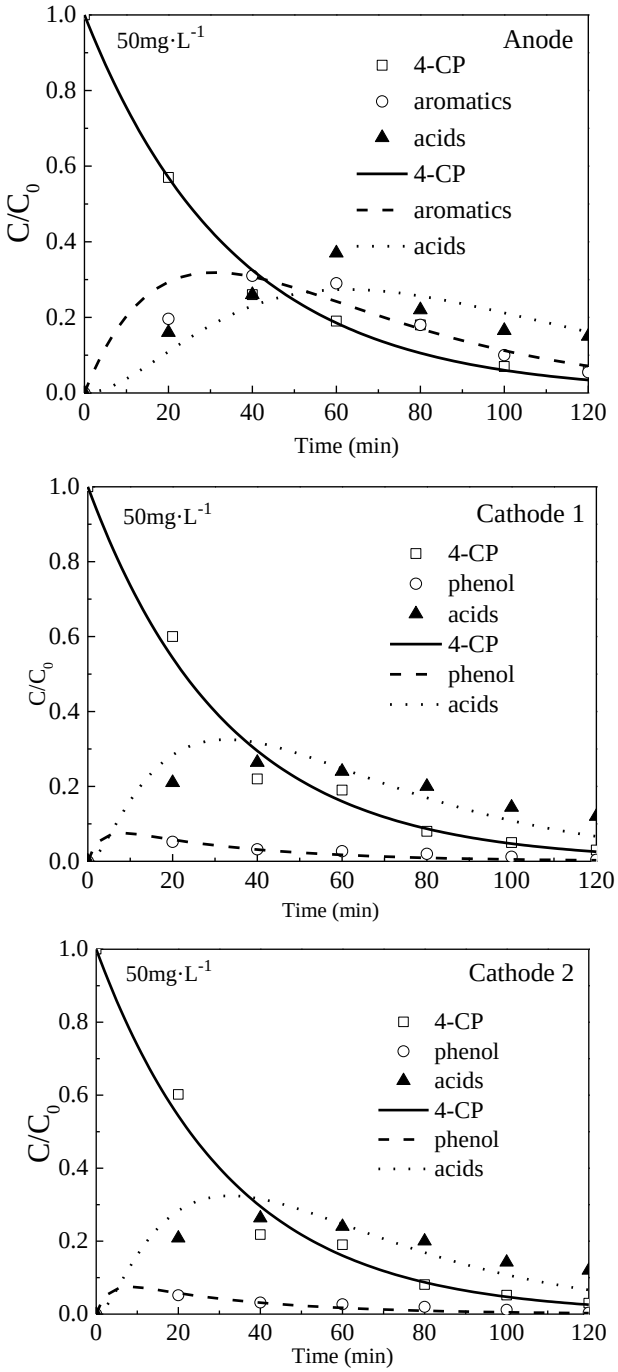

Fig. S3 Experimental data (symbols) and model-fitting (lines) results of 4-CP, aromatics (phenol) and acids with electrolysis time during electrochemical reduction-oxidation process in two cathodic and anodic compartments. Initial concentration: 50 mg L^{-1}. Current density: 25 mA cm^{-2}. Electrolyte: 0.03 mol L^{-1} Na_2SO_4. Initial pH: 7.0

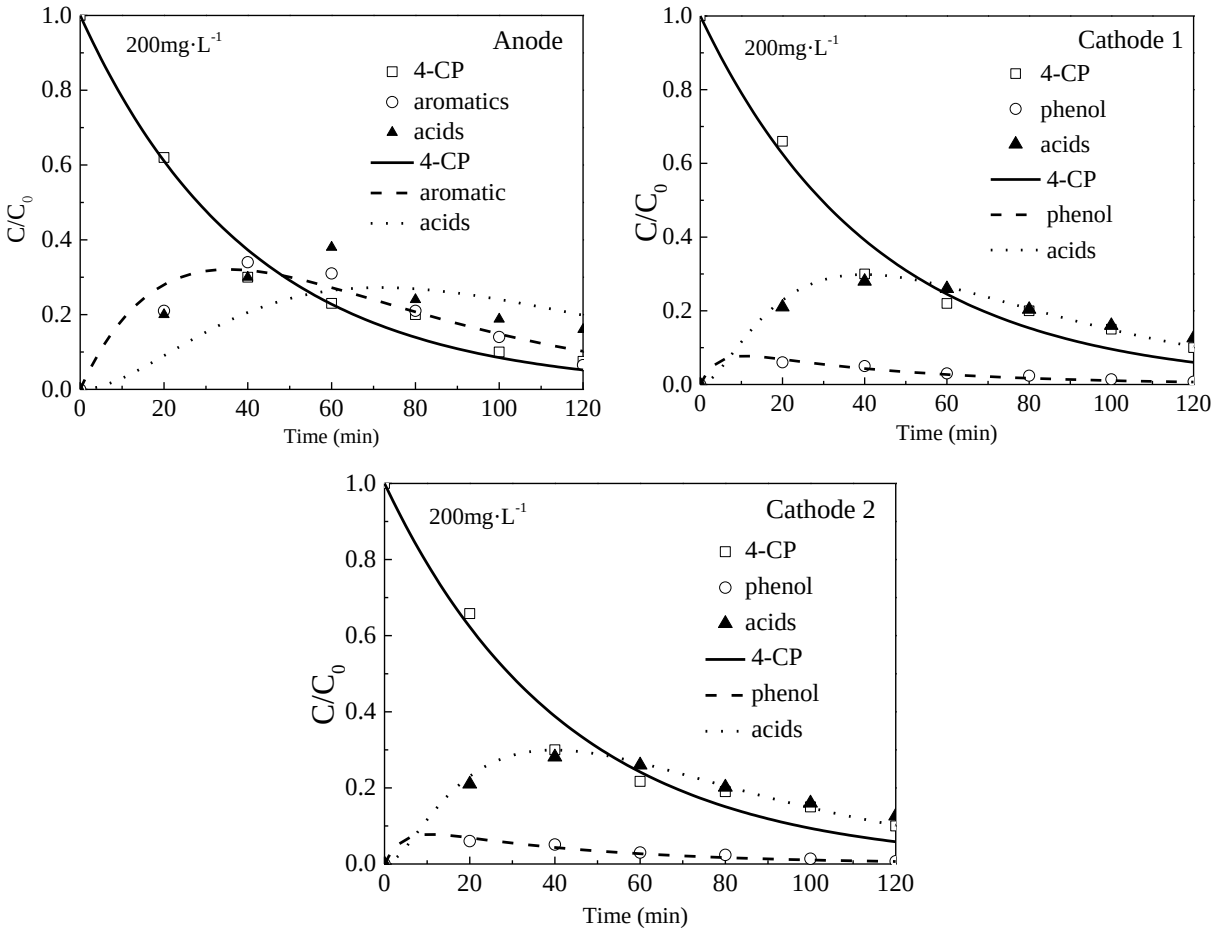

Fig. S4 Experimental data (symbols) and model-fitting (lines) results of 4-CP, aromatics (phenol) and acids with electrolysis time during electrochemical reduction-oxidation process in two cathodic and anodic compartments. Initial concentration: 200 mg L^{-1}. Current density: 25 mA cm^{-2}. Electrolyte: 0.03 mol L^{-1} Na_2SO_4. Initial pH: 7.0

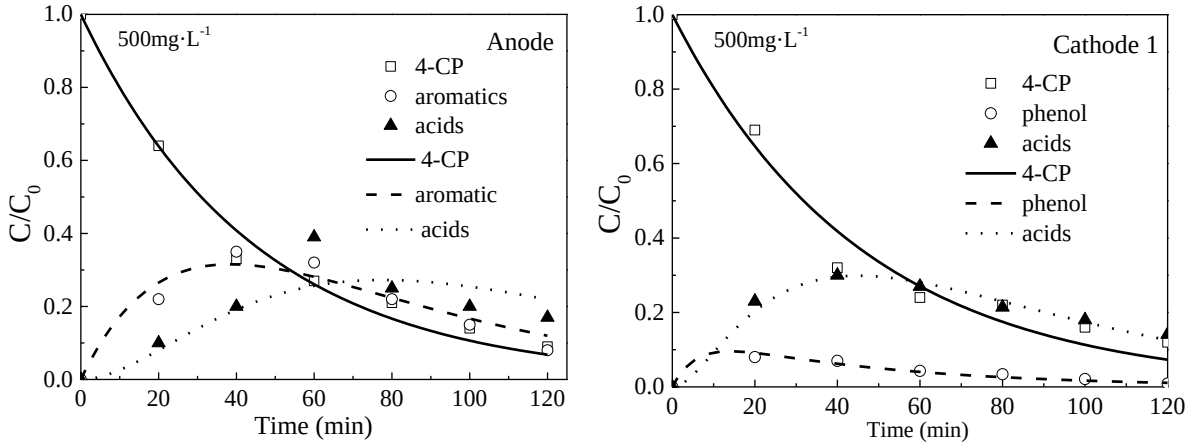

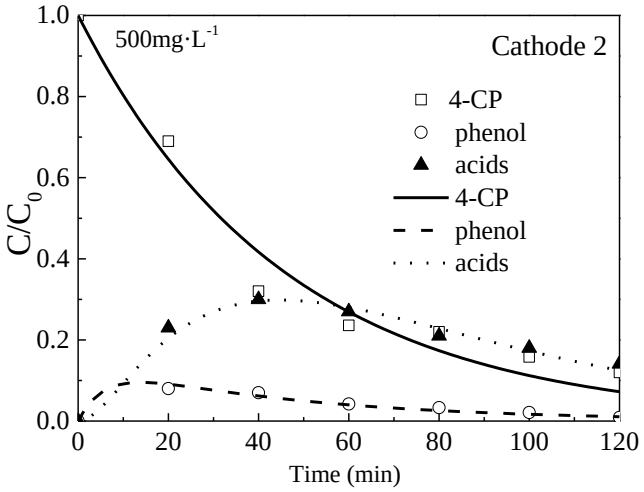

Fig. S5 Experimental data (symbols) and model-fitting (lines) results of 4-CP, aromatics (phenol) and acids with electrolysis time during electrochemical reduction-oxidation process in two cathodic and anodic compartments. Initial concentration: 500 mg L^{-1}. Current density: 25 mA cm^{-2}. Electrolyte: 0.03 mol L^{-1} Na_2SO_4. Initial pH: 7.0

Table S1. Fitting equations in the kinetics study and values of the correlation coefficient in anodic, cathodic 1 and cathodic 2 compartments with initial concentration of 100 mg L^{-1} 4-CP

	Compartment	Fitting equation	R^2
K_1	Anodic	$y=0.8609e^{-0.024x}$	0.981
	Cathodic 1	$y=0.9458e^{-0.028x}$	0.982
	Cathodic 2	$y=0.9449e^{-0.028x}$	0.982
K_2	Anodic	$y=4.129(e^{-0.028x}-e^{-0.035x})$	0.994
	Cathodic 1	$y=0.0975(e^{-0.031x}-e^{-0.324x})$	0.986
	Cathodic 2	$y=0.0965(e^{-0.029x}-e^{-0.328x})$	0.981
K_3	Anodic	$y=-2.280e^{-0.019x}+1.846e^{-0.054x}-4.122e^{-0.034x}$	0.986
	Cathodic 1	$y=-2.756e^{-0.031x}+0.1130e^{-0.318x}-2.869e^{-0.099x}$	0.998
	Cathodic 2	$y=-3.089e^{-0.029x}+0.1093e^{-0.328x}-3.198e^{-0.039x}$	0.998

Table S2 Estimate apparent kinetics constant K_i values obtained in the fit of experiments in anodic, cathodic 1 and cathodic 2 compartments with initial concentration of 25 mg L^{-1} 4-CP

K	Anodic	Cathodic 1	Cathodic 2
K_1	0.0297	0.0322	0.0322
K_2	0.0458	0.379	0.381
K_3	0.0349	0.0427	0.0449

Table S3 Estimate apparent kinetics constant K_i values obtained in the fit of experiments in anodic, cathodic 1 and cathodic 2 compartments with initial concentration of 50 mg L^{-1} 4-CP

K	Anodic	Cathodic 1	Cathodic 2
K_1	0.0285	0.0311	0.0304
K_2	0.0371	0.316	0.318
K_3	0.0314	0.0380	0.0384

Table S4 Estimate apparent kinetics constant K_i values obtained in the fit of experiments in anodic, cathodic 1 and cathodic 2 compartments with initial concentration of 200 mg L^{-1} 4-CP

K	Anodic	Cathodic 1	Cathodic 2
K_1	0.0246	0.0230	0.0237
K_2	0.0322	0.235	0.235
K_3	0.0271	0.0340	0.0343

Table S5 Estimate apparent kinetics constant K_i values obtained in the fit of experiments in anodic, cathodic 1 and cathodic 2 compartments with initial concentration of 500 mg L^{-1} 4-CP

K	Anodic	Cathodic 1	Cathodic 2
K_1	0.0224	0.0218	0.0219
K_2	0.0300	0.168	0.169
K_3	0.0254	0.0314	0.0315

ACKNOWLEDGEMENTS

This work was supported by Beijing Natural Science Foundation (No. 8172035), and the National Natural Science Foundation of China (No. 51278053 and 21373032).

References

1. N. Jaafarzadeh, F. Ghanbari, M. Ahmadi, M. Omidinasab, *Chem Eng J*, 308 (2017) 142.
2. G. W. Muna, N. Tasheva and G.M. Swain, *Environ Sci Technol*, 38 (2004) 3674.
3. S. W. Zhou, C. B. Zhang, X. F. Hu, Y. H. Wang, R. Xu, C. H. Xia, H. Zhang, Z. G. Song, *Appl Clay Sci*, 95 (2014) 275.
4. Y. H. Wang, K. Y. Chan, X.Y. Li, S. K. So, *Chemosphere*, 65 (2006) 1087.
5. M. Munoz, M. Kaspereit, B. J. M. Etzold, *Chem Eng J*, 285 (2016) 228.
6. F. Duan, Y. Z. Yang, Y. P. Li, H. B. Cao, Y. Wang, Y. Zhang, *J Environ Sci*, 26 (2014) 1171.
7. T. Ndlovu and O. A. Arotiba, *Int J Electrochem Sci*, 10 (2015) 8224.
8. M. P. Titus, V. G. Molina, M. A. Baños, J. Giménez, S. Esplugas, *Appl Catal B-Environ*, 47 (2004) 29.
9. M. S. Lucas, J. A. Peres, C. Amor, L. Prieto-Rodríguez, M. I. Maldonado, S. Malato, *J Hazard Mater*, 225–226 (2012) 173.
10. K. Eskelinen, H. Särkkä, T. A. Kurniawan, M. E. T. Sillanpää, *Desalination*, 255 (2010) 179.
11. C. A. Martínez-Huitle, M. A. Rodrigo, I. Sirés, O. Scialdone, *Chem Rev*, 115 (2015) 13362.
12. T. X. H. Le, M. Bechelany, S. Lacour, N. Oturan, M. A. Oturan, M. Cretin, *Carbon*, 94 (2015) 1003.
13. D. Gümüş and F. Akbal, *Process Saf Environ*, 103 (2016) 252.

14. I. Sirés, E. Brillas, M. Oturan, M. Rodrigo, M. Panizza, *Environ Sci Pollut Res*, 21 (2014) 8336.
15. H. Olvera-Vargas, N. Oturan, E. Brillas, D. Buisson, G. Esposito, M. A. Oturan, *Chemosphere*, 117 (2014) 644.
16. G. Chen, Z. Y. Wang and D. G. Xia, *Electrochim Acta*, 50 (2004) 933.
17. H. Wang, Z.Y. Bian, G. Lu, L. Pang, Z.P. Zeng, D. Z. Sun, *Appl Catal B-Environ*, 125 (2012) 449.
18. V. Sáez, M. D. E. Vicente, A. J. Frias-Ferrer, P. Bonete, J. Gonzalez-Garcia, *Water Res*, 43 (2009) 2169.
19. X. H. Mao, A. Ciblak, M. Amire, A. N. Alshawabken, *Environ Sci Technol*, 45 (2011) 6517.
20. S. L. Liu, H. Wang, Z.Y. Bian, *Water Sci Technol*, 71 (2015) 22.
21. C. Sun, S. A. Baig, Z. Lou, J. Zhu, Z. X. Wang, X. Li, J. H. Wu, Y. F. Zhang, X. H. Xu, *Appl Catal B-Environ*, 158-159 (2014) 38.
22. C. B. Molina, A. H. Pizarro, J. A. Casas, J. J. Rodriguez, *Appl Catal B-Environ*, 148 (2014) 330.
23. H. J. Luo, C. L. Li, C. Q. Wu, W. Zheng, X. Q. Dong, *Electrochim Acta*, 186 (2015) 486.
24. C. Brinzila, L. Ciríaco, M. J. Pacheco, A. Lopes, R. C. Ciobanu, *Adv Eng Forum*, 8 (2013) 370.
25. D. Vlastos, M. Antonopoulou and I. Konstantinou, *Sci Total Environ*, 551-552 (2016) 649.
26. D. Pokhrel and T. Viraraghavan, *Sci Total Environ*, 333 (2004) 37.
27. X. Z. Song, Q. Shi, H. Wang, S. L. Liu, C. Tai, Z. Y. Bian, *Appl Catal B-Environ*, 203 (2016) 442.
28. Q. Han, H. J. Wang, W. Y. Dong, T. Z. Liu, Y. L. Yin, H. F. Fan, *Chem Eng J*, 262 (2015) 34.
29. A. Karci, *Chemosphere*, 99 (2014) 1.
30. R. Daghrir, A. Dimboukou-Mpira, B. Seyhi, P. Drogui, *Sci Total Environ*, 490 (2014) 223.
31. M. Faust, R. Altenburger, T. Backhaus, H. Blanck, W. Bödeker, P. Gramatic, V. Hamer, M. Scholze, M. Vighi, L. H. Grimme, *Aquat Toxicol*, 63 (2003) 43-63.
32. Y. Liu, L. Liu, J. Shan, J. D. Zhang, *J Hazard Mater*, 290 (2015) 1.
33. I. Sirés, J. A. Garrido, R. M. Rodríguez, E. Brillas, N. Oturan, M. A. Oturan, *Appl Catal B-Environ*, 72 (2007) 382.
34. Y. Wang, Q. Shi, H. Wang, Z. Y. Bian, *Environ Sci*, 37 (2015) 1437 (in Chinese).
35. Z. C. Wu and M. H. Zhou, *Environ Sci Technol*, 35 (2001) 2698.
36. E. Illés, E. Szabó, E. Takács, L. Wojnárovits, A. Dombi, K. Gajda-Schrantz, *Sci Total Environ*, 472 (2014) 178.
37. M. M. Zheng, J. G. Bao, P. Liao, K. Wang, S. H. Yuan, M. Tong, H. Y. Long, *Chemosphere*, 87 (2012) 1097.
38. A. Z. Li, X. Zhao, Y. N. Hou, H. J. Liu, L. Y. Wu, J. H. Qu, *Appl Catal B-Environ*, 111-112 (2012) 628.
39. F. He, L. C.Lei, *J Zhejiang Univ Sci*, 5 (2004) 198.
40. M. H. Zhou, Z. C. Wu, X. J. Ma, Y. Q. Cong, Q. Ye, D. H. Wang, *Sep Purif Technol*, 34 (2004) 81.
41. Y. S. Shen, Y. Ku, K. C. Lee, *Water Res*, 29 (1995) 907.
42. S. O. Ko, D. H. Lee, Y. H. Kim, *Environ Technol*, 28 (2007) 583.
43. W. S. Kuo, *Chemosphere*, 39 (1999) 1853.